JOURNAL OF NATURAL PRODUCTS

pubs.acs.org/jnp

Note

Bioactive Cyclodepsipeptides from Cocultured Mangrove-Derived *Aspergillus* sp. and *Penicillium* sp.

Yu Wang, Guang-Ping Cao, Xin-Jian Qu, Yong-Hong Liu, Xiang-Xi Yi, Cheng-Hai Gao,* and Meng Bai*

Cite This: *J. Nat. Prod.* 2025, 88, 2239−2246

Read Online

ACCESS | Metrics & More | Article Recommendations | Supporting Information

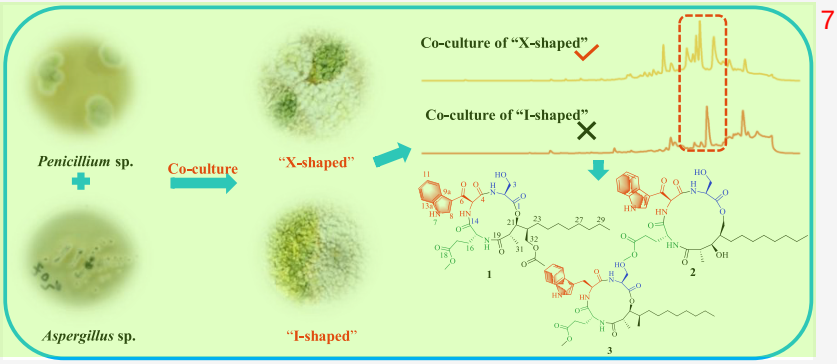

ABSTRACT: Three new arthrichitin derivatives I−K (**1**−**3**) and three known congeners (**4**−**6**) were isolated from a coculture of mangrove-derived fungi *Aspergillus* sp. and *Penicillium* sp. using ^{1}H NMR-guided fractionation. Their structures were determined by comprehensive spectroscopic analysis (1D/2D NMR, HRESIMS, ESI-MS/MS), Marfey's analysis, DP4+ probability, and experimental/computed ECD comparison. All compounds were evaluated for antibacterial effects and cytotoxicity. Notably, compounds **1** and **5** showed weak cytotoxicity against MHCC-97H cells (IC_{50} = 20.1 ± 0.9 and 25.8 ± 0.4 μM, respectively). Compound **4** exhibited potent anti-BPH activity (IC_{50} = 0.36 ± 0.02 μM).

Fungi are invaluable sources of natural products, yielding structurally novel secondary metabolites (SMs) with wide-ranging bioactivities, making them crucial for drug discovery and biotechnology.[1,2] Recent data reveal a striking predominance of fungal-derived natural products over bacterial counterparts, with the ratio increasing from 2.4:1 (2020) to 4.4:1 (2022), underscoring the exceptional potential of fungal resources in natural product discovery.[3] Nevertheless, conventional laboratory cultivation methods often fail to mimic native microbial community interactions, potentially restricting the biosynthetic output of fungal SMs.[4] Despite extensive exploration of fungal SMs the field now contends with high rediscovery rates of known compounds and diminishing returns in identifying structurally novel bioactive molecules.[5,6]

Over the past decade, numerous innovative strategies have emerged to activate silent biosynthetic pathways in fungi, among which coculture techniques have proven particularly effective for inducing novel metabolite production via genetic regulatory mechanisms.[7] Microbial coculture involves the cultivation of two or more microbial strains within a shared, controlled environment. Optimized coculture systems demonstrate enhanced stability, robustness, and functional performance relative to conventional monoculture approaches.[8] Currently, most coculture studies focus on strains from completely different environments, while coculturing microorganisms from the same or similar habitats remains a worthwhile direction with unforeseen implications.[9,10]

In previously published works, we described isolation and identification of four new cyclic pentapeptides avellanins D−G from the mangrove-derived fungus *Aspergillus* sp. GXIMD 03099,[11,12] and a new cyclic heptapeptide cadophorin C together with a known analogue cadophorin B from the mangrove-derived *Penicillium* sp. GXIMD 03101.[13] To better explore their ability to produce structurally novel cyclic peptide SMs, we investigated the SMs produced by their coculture.

A review of the fungal coculture literature reveals that studies explicitly reporting inoculation methods typically employ two distinct patterns: linear and cross inoculation.[14−18] Notably, no direct comparisons between these inoculation methods typically appear to have been made, which prompted us to investigate whether enhanced interfacial contact through different inoculation geometries would differentially regulate SMs. To test this hypothesis, *Aspergillus* sp. GXIMD 03099

Received: June 17, 2025
Revised: August 16, 2025
Accepted: August 25, 2025
Published: September 2, 2025

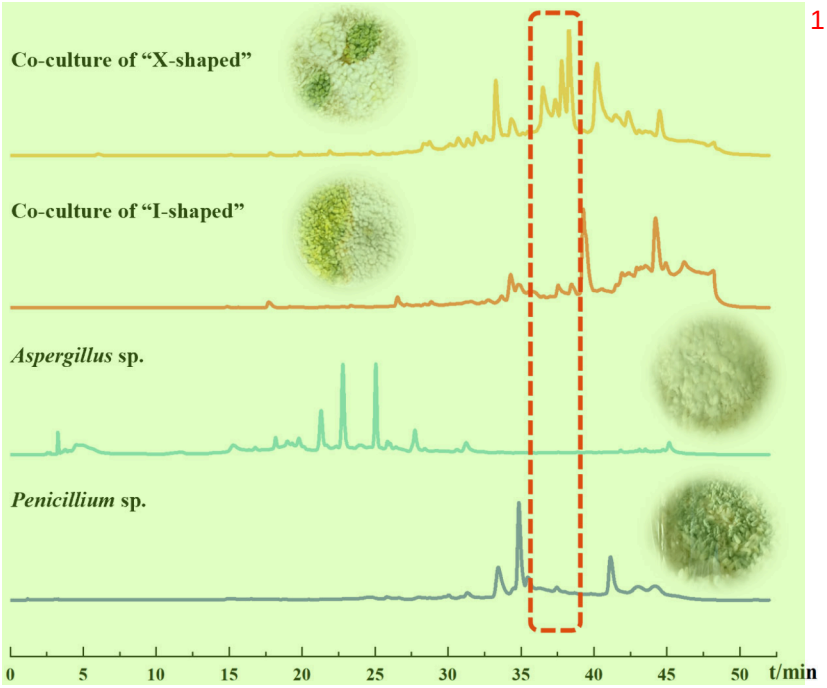

Figure 1. HPLC analysis of extracts from *Aspergillus* sp. GXIMD 03099, *Penicillium* sp. GXIMD 03101, and their Coculture (including "X-shaped" and "I-shaped").

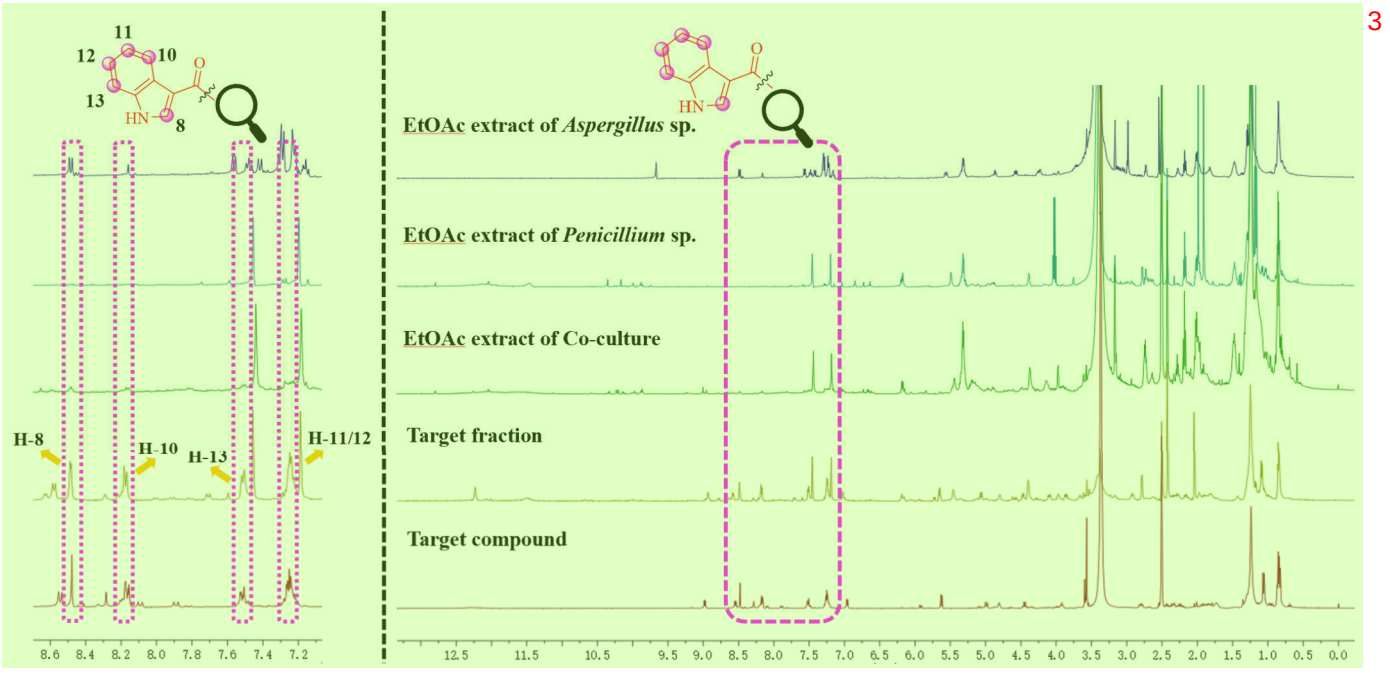

Figure 2. ^{1}H NMR spectra of the EtOAc extract, the target fraction, and a target compound from the fungus *Aspergillus* sp. GXIMD 03099, *Penicillium* sp. GXIMD 03101, and Coculture.

and *Penicillium* sp. GXIMD 03101 were cocultured using both linear (single-line, "I-shaped") and cross ("X-shaped") inoculation methods. Comparative HPLC-DAD analysis of SMs revealed significant differences in metabolite profiles between the X-shaped and I-shaped systems (Figure 1). The X-shaped approach exhibited greater chemical diversity, likely attributable to its expanded contact interface, potentially facilitating enhanced metabolic exchange between the species. Based on these findings, the subsequent coculture fermentations in this study were performed using the X-shaped inoculation approach.

Comparative analysis of the ^{1}H NMR spectra (Figure 2) between monoculture and cross-shaped coculture metabolites revealed significantly enhanced spectral complexity in the ethyl acetate extract of cocultured fungi. The coculture extract exhibited numerous additional resonance peaks absent in monoculture samples, indicating the potential presence of novel metabolites. Further analysis of the coculture metabolite ^{1}H NMR spectra revealed characteristic signals indicative of a

https://doi.org/10.1021/acs.jnatprod.5c00752
J. Nat. Prod. 2025, 88, 2239−2246

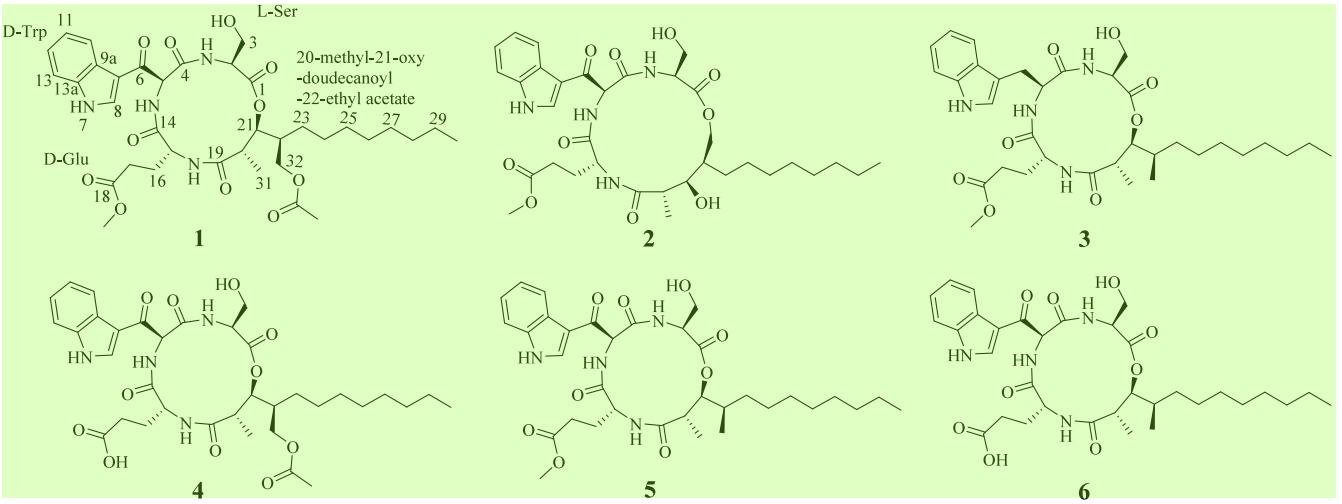

1

tryptophan moiety, notably including a singlet corresponding to the NH proton of the indole nitrogen (δ_H ~8.48, s, H-8) and four mutually coupled aromatic protons (δ_H ~7.23, m, H-11/12; ~7.51, m, H-13; ~8.17, m, H-10).[19,20] Based on these diagnostic NMR signatures, we developed a targeted NMR-guided isolation protocol for tryptophan-containing derivatives. This methodology enabled the successful isolation and structural elucidation of six arthrichitin derivatives, including three previously undescribed arthrichitin analogs arthrichitins I−K (**1**−**3**). Additionally, the antibacterial activity, cytotoxic activity and benign prostatic hyperplasia (BPH) inhibitory activities of these arthrichitin derivatives were evaluated. Herein, the isolation, structure elucidation, and bioactivities of compounds **1**−**3** are described. 2

Compound **1** was isolated as light-yellow powder and assigned the molecular formula $C_{36}H_{50}N_4O_{11}$ based on HRESIMS ($[M + Na]^+$ at m/z 737.3370, as well as indicated the presence of 14 degrees of unsaturation (Figure S8). Carefully analysis of the ^{1}H NMR and HSQC spectra (Table 1, Figure S1 and S4) revealed the presence of a free hydroxy group [δ_H 4.82, (t, J = 5.0 Hz)], three amide protons [δ_H 9.00 (d, J = 6.5 Hz), 8.60 (d, J = 7.5 Hz), and 6.98 (d, J = 6.0 Hz)], five aromatic protons [δ_H 8.48 (s), 8.17 (dd, J = 7.0, 2.0 Hz), 7.51 (d, J = 7.0 Hz), 7.24 (m), and 7.24 (m)], and four methyl protons [δ_H 3.57 (s), 2.04 (s), 1.08 (d, J = 7.0 Hz), and 0.85 (t, J = 6.0 Hz)]. The spectrum also displayed three α-amino protons [δ_H 5.63 (d, J = 6.5 Hz), 4.46 (q, J = 7.5 Hz), and 3.94 (m)], indicative of three amino acid residues within this structure. The ^{13}C NMR and DEPT spectrum exhibited 36 carbon signals (Table 1, Figure S2 and S3), including seven carbonyl carbon signals (δ_C 185.0, 174.7, 172.6, 171.9, 170.5, 169.1, and 167.5), eight sp^2-hybridized carbons (δ_C 137.1, 136.7, 125.6, 123.4, 122.5, 121.2, 113.5, and 112.6), six methines [including three α-amino carbons (δ_C 62.1, 55.0, and 51.9), one oxygenated (δ_C 76.3), δ_C 41.4, and 38.0], 11 methylenes (including two oxygenated), along with four methyls (δ_C 51.4, 20.8, 16.1, and 14.0). Additionally, a broad singlet at δ_H 12.27 (NH) and the observed sp^2 carbon chemical shifts suggested the presence of an indole moiety. Further analysis confirmed the presence of one serine (Ser), one glutamic acid (Glu), and one modified fatty acid with an oxygen-bound carbon (δ_C 76.3). The amino acid sequence was unambiguously determined through comprehensive analysis of ^{1}H−^{1}H COSY, HMBC, and NOESY correlation spectra (Figure 3, S5, S6, and S7). There are four spin systems 3

supported by the ^{1}H−^{1}H COSY interactions of H-2/H-3, H-10/H-11/H-12/H-13, H-16/H-17, and H-20/H-21/H-22/H-23/H-24/H-25/H-26/H-27/H-28/H-29/H-30. The key sequential connectivity was established as follows: the α-proton (δ_H 3.94, H-2) and 2-NH (δ_H 6.98) of Ser exhibited a distinct HMBC correlation to the carbonyl carbon (δ_C 167.5, C-4) of Trp, while the α-proton (δ_H 5.63, H-5) and 5-NH (δ_H 9.00) of Trp showed connectivity to the carbonyl carbon (δ_C 171.9 C-14) of Glu, thereby confirming the partial sequence Ser-Trp-Glu. Further sequence extension to Ser-Trp-Glu-fatty acid were evidenced by the HMBC correlations from H-15 (δ_H 4.46) and 15-NH (δ_H 8.60) to C-19 (δ_C 174.7). and H-21 (δ_H 5.05) to C-1 (δ_C 169.1) (Figure 3). Finally, NOESY correlations between the α-protons of Ser, Trp, Glu, and fatty acid, the ESI-MS/MS fragment ions at m/z 430 (loss of fatty acid), and m/z 287 (loss of Glu) (Figure 3 and S7), and combined with degree of unsaturation analysis, unambiguously demonstrated cyclization through an amide/ester bond between Ser, Trp, Glu, and fatty acid residues, forming the observed macrocyclic peptide structure (Figure 3). Thus, the planar structure of **1** was elucidated as a cyclodepsipeptide containing a 4-(acetoxymethyl)-3-hydroxy-2-methyldodecanoic acid moiety. 4

The absolute configurations of the two natural acids (Glu and Ser) in **1** were determined by HPLC-MS analysis of their acid hydrolysates following derivatization with Marfey's reagent.[21] The results showed that the Glu and Ser were identified as D-Glu and L-Ser (Figure S13). Furthermore, the spectroscopic data of **1** closely matched those of arthrichitin E (**4**), differing only by an additional methyl group. This structural assignment was further corroborated by the HMBC correlation from -OCH$_3$ (δ_C 51.4 and δ_H3.57) to C-18. Considering the configuration of fatty acid, which was presence of three consecutive stereocenters at C-20/C-21/C-22. Previous studies have demonstrated that the J-coupling constants of the trisubstituted dodecanoic acid moiety at C-10/C-21/C-22 serve as key diagnostic parameters for determining *anti* or *syn* configurations between contiguous chiral centers.[22,23] The large vicinal coupling constant between H-20 and H-21 (J = 9.5 Hz) indicated an *anti*-relationship between the contiguous chiral centers C-20 and C-21, while the small coupling constant (J = 1.5 Hz) between H-21 and H-22 suggested a *syn*-arrangement. This J-based configurational analysis established the relative configuration of **1** as 20*S**,21*S**,22*S**, which was also assigned by DP4+ calculations 5

https://doi.org/10.1021/acs.jnatprod.5c00752
J. Nat. Prod. 2025, 88, 2239−2246

Table 1. ^{1}H NMR (500 MHz) and ^{13}C NMR (125 MHz) Data (δ) for 1−3 in DMSO-d_6 (δ in ppm, J in Hz) 1

Residue	Position	1		2		3	2
		δ_C Type	δ_H (J in Hz)	δ_C Type	δ_H (J in Hz)	δ_C Type	δ_H (J in Hz)
L-Ser	1	169.1, C		169.3, C		169.2, C	
	2	55.0, CH	3.94, m	54.6, CH	4.39, m	54.2, CH	4.04, m
	3	59.0, CH_2	3.39, m	61.9, CH_2	3.66, m; 3.51, m	59.2, CH_2	3.54, m; 3.47, m
	-OH		4.82, t (5.0)		5.11, t (4.0)		4.83, brs
	-NH		6.98, d (6.0)		7.70, d (9.5)		7.24, d (6.5)
D-Trp	4	167.5, C		167.0, C		171.8, C	
	5	62.1, CH	5.63, d (6.5)	60.4, CH	5.71, d (7.0)	56.1, CH	5.63, d (6.5)
	6	185.0, C		186.1, C		26.4, CH_2	3.08, dd (14.5, 5.0); 2.99, dd (14.5, 4.5)
	-NH		12.27, brs		12.20, brs		10.80, s
	8	137.1, CH	8.48, s	137.3, CH	8.80, s	123.4, CH	7.14, d (2.0)
	9	113.5, C		114.3, C		110.3, C	
	9a	125.6, C		125.6, C		127.0, C	
	10	121.2, CH	8.17, dd (7.0, 2.0)	121.2, CH	8.18, dd (7.0, 2.0)	117.9, CH	7.51, d (8.0)
	11	122.5, CH	7.24, m	122.3, CH	7.24, m	118.3, CH	6.97, d (8.0)
	12	123.4, CH	7.24, m	123.3, CH	7.24, m	120.9, CH	7.06, d (8.0)
	13	112.6, CH	7.51, d (7.0)	112.5, CH	7.50, d (7.0)	111.4, CH	7.32, d (8.0)
	13a	136.7, C		136.7, C		136.1, C	
	-NH		9.00, d (6.5)		8.80, d (7.0)		8.62, d (8.5)
D-Glu	14	171.9, C		172.0, C		171.6, C	
	15	51.9, CH	4.46, q (7.5)	52.7, CH	4.34, q (7.5)	51.7, CH	4.20, q (8.0)
	16	25.0, CH_2	1.82, m	25.5, CH_2	1.85, m	24.7, CH_2	1.74, m
	17	29.8, CH_2	2.44, m; 2.36, m	29.5, CH_2	2.41, m; 2.18, m	29.5, CH_2	2.14, m; 2.17, m
	18	172.6, C		172.5, C		172.5, C	
	-NH		8.60, d (7.5)		8.63, d (6.0)		8.43, d (8.5)
	-OMe	51.4, CH_3	3.57, s	51.4, CH_3	3.53, s	51.4, CH_3	3.57, s
20-methyl-21-oxy-doudecanoyl-22-ethyl acetate	19	174.7, C		177.1, C		174.6, C	
	20	41.4, CH	2.91, dq (9.5, 7.0)	41.3, CH	2.58, dq (9.5, 7.0)	41.3, CH	2.75, dd (10.0, 7.0)
	21	76.3, CH	5.05, dd (9.5, 1.5)	76.2, CH	3.17, dd (10.5, 2.0)	78.1, CH	5.01, dd (10.0, 1.5)
	−OH				4.56, d (11.0)		
	22	38.0, CH	1.95, m	41.0, CH	1.76, m	33.2, CH	1.71, m
	23	28.4, CH_2	1.24, m	29.9, CH_2	1.26, m	33.4, CH_2	1.30, m; 1.06, m
	24	26.5, CH_2	1.42, m; 1.28, m	26.4, CH_2	1.33, m; 1.28, m	28.7, CH_2	1.25, m
	25	28.7, CH_2	1.24, m	28.8, CH_2	1.26, m	28.7, CH_2	1.25, m
	26	28.9, CH_2	1.24, m	29.1, CH_2	1.26, m	29.1, CH_2	1.25, m
	27	29.1, CH_2	1.24, m	29.2, CH_2	1.26, m	29.2, CH_2	1.25, m
	28	31.3, CH_2	1.26, m	31.4, CH_2	1.26, m	31.3, CH_2	1.25, m
	29	22.1, CH_2	1.26, m	22.1, CH_2	1.26, m	22.2, CH_2	1.25, m
	30	14.0, CH_3	0.85, t (6.0)	14.0, CH_3	0.84, t (7.0)	14.0, CH_3	0.86, t (7.0)
	31	16.1, CH_3	1.08, d (7.0)	15.6, CH_3	1.05, d (7.0)	16.1, CH_3	1.08, d (7.0)
	32	63.3, CH_2	4.09, m; 3.85, m	65.1, CH_2	4.26, m; 3.65, m	13.4, CH_3	0.81, d (6.5)
	33	170.5, C					
	34	20.8, CH_3	2.04, s				

with a probability of 97.59% (Figure S14). Given the previously determined absolute configurations of the amino acid constituents, we further confirmed the complete absolute configuration of **1** through ECD calculations. The calculated ECD spectra for (2*S*,5*S*,15*R*,20*S*,21*S*,22*S*)-**1** were exhibited the closest agreement with the experimental ECD data (Figure S15). This assignment was further corroborated by comparative CD spectroscopy, which showed that the CD spectrum of **1** (Figure S15) matched precisely with those reported for arthrichitins B−H in the literature.[19,20] 3

Furthermore, comparative analysis of optical rotation data revealed consistency between **1** ([α]24 D + 15.0, *c* 0.1, MeOH) and arthrichitins B−H,[19,20] suggesting a shared stereochemical configuration among of these compounds. Collectively, these results confirm that the absolute configuration of **1** as comprising: L-Ser, D-Trp, D-Glu, and 2*S*,4*S*-dimethyl-3*S*-oxidodecanoic acid, and named arthrichitin I. 4

Compound **2** was obtained as white powder. The molecular formula was established as $C_{34}H_{48}N_4O_{10}$ (13 degrees of unsaturation) based on HRESIMS analysis, which showed a 5

https://doi.org/10.1021/acs.jnatprod.5c00752
J. Nat. Prod. 2025, 88, 2239−2246

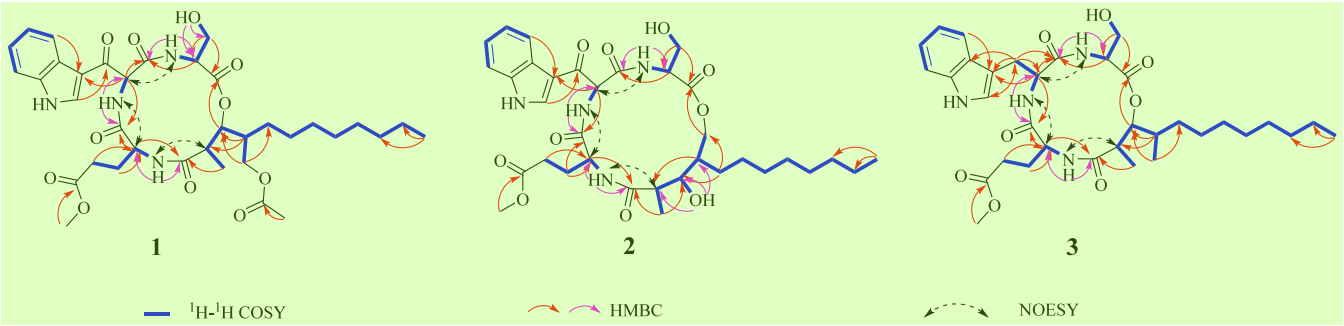

Figure 3. Key ^{1}H−^{1}H COSY, HMBC, and NOESY correlations for compounds **1**−**3**.

hydrogen adduct ion at *m*/*z* 673.3438 [M + H]$^+$ (calcd for 673.3449) (Figure S23). Analysis of the ^{1}H NMR spectrum (Figure S16) of **2** revealed the presence of two free hydroxy groups [δ_H 5.11 (t, *J* = 4.0 Hz) and 4.56 (d, *J* = 11.0 Hz)], three amide protons [δ_H 8.80 (d, *J* = 7.0 Hz), 8.63 (d, *J* = 6.0 Hz), and 7.70 (d, *J* = 9.5 Hz)], five aromatic protons [δ_H 8.48 (s), 8.18 (dd, *J* = 7.0, 2.0 Hz), 7.50 (d, *J* = 7.0 Hz), 7.24 (m), and 7.24 (m)], and three methyl protons [δ_H 3.53 (s), 1.05 (d, *J* = 7.0 Hz), and 0.84 (t, *J* = 7.0 Hz)]. The spectrum also displayed three α-amino protons [δ_H 5.71 (d, *J* = 7.0 Hz), 4.39 (m), and 4.34 (q, *J* = 7.5 Hz)]. Additionally, the ^{13}C NMR and DEPT spectrum exhibited 34 carbon signals (Table 1, Figures S17 and S18), including six carbonyl carbon signals (δ_C 186.1, 177.1, 172.5, 172.0, 169.3, and 167.0), eight sp^2-hybridized carbons (δ_C 137.3, 136.7, 125.6, 123.3, 122.3, 121.2, 114.3, and 112.5), six methines (including three α-amino carbons and one oxygenated), 11 methylene (two oxygenated), along with four methyl. Based on the characteristic UV spectrum (Figure S25) and NMR data, which were highly analogous to those of **1**, the only obvious difference was the acetyl group at C-32 had been replaced by a hydroxyl group. Detailed analysis of the 1D NMR data for compounds **2** and **1** revealed that the resonance of C-32 shifted to downfield from δ_C 63.3 in **1** to 65.1 in **2**, while the resonance of C-22 shifted to upfield from δ_C 38.0 in **1** to 41.0 in **2** and C-23 from δ_C 28.4 in **1** to 29.9 in **2**. These spectroscopic features suggested that an ester linkage was established between the C-32 hydroxymethyl and C-1 carbonyl moieties in **2**, which was supported by the COSY and HMBC data (Figure 3, Figures S20 and S21). The ^{1}H−^{1}H COSY cross-peaks of H-21 and 21-OH. Furthermore, the HMBC correlations from 21-OH to C-19, C-20, and C-21; and from H-21 to C-1, C-21, C-22, and C-23 further supported the preceding structural assignment. Thus, the planar structure of compound **2** was established, and the absolute configurations of **2** was determined by Marfey's analysis, DP4+ calculations, and experimental ECD spectrum (Figures S28, S29, and S30). Finally, the structure of **2** was elucidated as $_L$-Ser, $_D$-Trp, $_D$-Glu, and 2*S*,4*R*-dimethyl-3*S*-oxidodecanoic acid, and named as arthrichitin J.

Compound **3** was isolated as light-yellow powder. Its molecular formula was determined to be $C_{34}H_{50}N_4O_8$ (12 degrees of unsaturation) by HRESIMS analysis, which displayed a hydrogen adduct ion peak at *m*/*z* 643.3698 [M + H]$^+$ (calcd for 643.3707) (Figure S38). Analysis of the ^{1}H NMR spectrum (Figure S31) of **3** revealed the presence of a free hydroxy groups [δ_H 4.83 (brs)], three amide protons [δ_H 8.62 (d, *J* = 8.5 Hz), 8.43 (d, *J* = 8.5 Hz), and 7.24 (d, *J* = 6.5 Hz)], five aromatic protons [δ_H 7.51 (d, *J* = 8.0 Hz), 7.32 (d, *J* = 8.0 Hz), 7.14 (d, *J* = 2.0 Hz), 7.06 (d, *J* = 8.0 Hz), and 6.97 (d, *J* = 8.0 Hz)], and four methyl protons [δ_H 3.57 (s), 1.08 (d, *J* = 7.0 Hz), 0.86 (t, *J* = 7.0 Hz), and 0.81 (d, *J* = 6.5 Hz)]. The spectrum also displayed three α-amino protons [δ_H 5.63 (d, *J* = 6.5 Hz), 4.20 (q, *J* = 8.0 Hz), and 4.04 (m)]. Additionally, the ^{13}C NMR and DEPT spectrum exhibited 34 carbon signals (Table 1, Figures S32 and S33), including five carbonyl carbon signals (δ_C 174.6, 172.5, 171.8, 171.6, and 169.2), eight sp^2-hybridized carbons (δ_C 136.1, 127.0, 123.4, 120.9, 118.3, 117.9, 111.4, and 110.3), six methines (including three α-amino carbons and one oxygenated), 11 methylene (one oxygenated), along with four methyl. Based on the characteristic UV spectrum (Figure S40) and NMR data, which were highly analogous to those of **5**, the major differences were the chemical shifts of C-6 (δ_C 184.9 in **5** vs δ_C 26.4 in **3**) and H-6 (missing in **5** vs δ_H 3.08/2.99 in **3**), suggesting the carbonyl group at C-6 had been hydrogenated to a methylene group, which was supported by the COSY and HMBC data (Figure 3, Figure S35, and S36). The ^{1}H−^{1}H COSY cross-peaks of H-5, H-6, and 5-NH. Moreover, the HMBC correlations from H-6 to C-4, C-5, C-7, C-8, and C-9a further supported the preceding structural assignment. Consequently, the planar structure of **3** was full established. The absolute configurations of **3** was deduced to be the same as those of **1** and **2** according to the Marfey's analysis, DP4+ calculations, and experimental ECD spectrum (Figures S43, S44, and S45). Additionally, the structural assignment was further supported by biogenetic considerations and negative optical rotations. Finally, the structure of **3** was elucidated and named as arthrichitin K.

Three known compounds, arthrichitin E (**4**),[19] arthrichitin C (**5**),[20] and arthrichitin (**6**),[20] were identified by comparison of their physical and spectroscopic data with literature reports.

Compounds **1**−**6** were evaluated for antimicrobial activity and cytotoxicity. Additionally, compounds **1**, **4**, and **6** were assessed for inhibitory activity against benign prostatic hyperplasia (BPH). The results indicated that compounds **1** and **5** exhibited weak cytotoxicity against the MHCC-97H cell line, with IC_{50} values of 20.1 ± 0.9 μM and 25.8 ± 0.4 μM, respectively. Compound **1** also showed weak cytotoxicity against KTC-1 cell line (IC_{50} = 27.4 ± 0.1 μM). Cisplatin, used as a positive control, with the IC_{50} values of 4.6 ± 0.2 μM (against MHCC-97H) and 19.3 ± 0.3 μM (against KTC-1), respectively. Compound **6** displayed a zone of inhibition against *Bacillus subtilis* measuring 3.52 ± 0.12 mm in diameter, while chloromycetin (positive control) yielded a zone of 5.74 ± 0.08 mm in diameter. Notably, compound **4** demonstrated significant inhibitory activity against BPH, with an IC_{50} value of 0.36 ± 0.02 μM, outperforming the positive control finasteride (IC_{50} value of 0.49 ± 0.04 μM).

https://doi.org/10.1021/acs.jnatprod.5c00752
J. Nat. Prod. 2025, 88, 2239−2246

In conclusion, we reported three new arthrichitin derivatives named arthrichitins I–K (**1**–**3**). The key structural distinction among compounds **1**–**3** lies in the cyclization pattern of compound **2**, which undergoes dehydration at the C-32 position to form the ring. The biological activity screening showed that only compounds **1**, and **4**–**6** had antibacterial activity, cytotoxic activity, and inhibitory activity against BPH, respectively.

EXPERIMENTAL SECTION

General Experimental Procedures. Optical rotation measurements were acquired using an InsMark digi300 polarimeter. Circular dichroism (CD) spectral analyses were conducted on a JASCO J-1500 digital polarimeter. Infrared spectroscopic data were collected with a PerkinElmer DTGS FT/IR-L1600400 spectrophotometer employing KBr pellets. Nuclear magnetic resonance (NMR) experiments including both 1D and 2D spectra were recorded on Bruker AV-400 (400 MHz) and AV-500 (500 MHz) spectrometers, with tetramethyl silane (TMS) serving as the internal reference. Semi-preparative HPLC separations were achieved using a Shimadzu LC-2030C system equipped with a DAD detector and a COSMOSIL $5C_{18}$-MS-II column (10 mm i.d. × 250 mm length, 7 μm particle size). Melting points were determined using an SGW X-4B micromelting apparatus without calibration. HR-ESI-MS was obtained on two instruments: a Bruker Daltonics Apex-Ultra 7.0 T FT-ICR MS and a Waters Q-TOF Ultima Global GAA076 LC/MS system.

Fungal Material. The fungal strains *Aspergillus* sp. GXIMD 03099 (GenBank accession No. ON668102) and *Penicillium* sp. GXIMD 03101 (GenBank accession No. MZ971181) were obtained from the mangrove plant *Acanthus ilicifolius* L. collected in July 2020 from Guangxi Shankou Mangrove Nature Reserve, China. Taxonomic identification combined morphological characterization with ITS region sequencing and Blastn analysis against the NCBI database. Both strains have been deposited in the Marine Culture Collection of the Institute of Marine Drugs, Guangxi University of Chinese Medicine, Nanning, China.

Fermentation and Isolation. The fungal strains *Aspergillus* sp. GXIMD 03099 and *Penicillium* sp. GXIMD 03101 were initially cultured on potato dextrose agar (PDA) for 3 days. Mycelial plugs were aseptically transferred to eight 500 mL Erlenmeyer flasks, each containing 200 mL of potato dextrose broth (PDB), and incubated at 37 °C under shaking conditions (180 rpm) for 3 days. Seed cultures (2 mL) were inoculated via the cross-streak method into rice-based medium [80 g rice, 100 mL distilled water, and 0.5 g sea salt per 1 L flask], followed by static cultivation at 25 °C for 30 days. The whole solid fermentation product of the fungi was dried and extracted with EtOAc (3 × 15L) to yield 120.1 g. Fractionation was carried out via silica gel (200–300 mesh) column chromatography (CC) employing stepwise gradients of petroleum ether (PE)/EtOAc (100:0 → 0:100, v/v) and subsequently EtOAc/MeOH (100:0 → 0:100, v/v), yielding 11 fractions (Fr.1–Fr.11).

Fr. 6 (18.57 g) was subjected to stepwise gradient elution of 10–100% MeOH/H_2O to give 21 subfractions, fractions 6–1–6–21. Fraction 6–17 (2.67 g) was further separated using with stepwise gradient elution of 10–100% MeOH/H_2O to give 9 subfractions, fractions 6–17–1–6–17–9. Subfraction 6–17–5 was further separated by semipreparative HPLC (MeOH/H_2O, 85:15, *v*/*v*) to obtain **1** (8.95 mg, t_R = 22.39 min). Subfraction 6–17–3 was further separated by semipreparative HPLC (MeOH/H_2O, 81:19, *v*/*v*) to obtain **2** (6.98 mg, t_R = 30.91 min). Subfraction 6–17–6 was further separated by semipreparative HPLC (MeOH/H_2O, 85:15, *v*/*v*) to obtain and **5** (3.58 mg, t_R = 53.84 min), **6** (8.54 mg, t_R = 36.35 min). Fr. Seven (1.47 g) was fractionated by semipreparative HPLC (MeOH/H_2O, 95:5, *v*/*v*) to give compound **4** (45.16 mg, t_R = 14.04 min). Fr. Nine (0.25 g) was fractionated by semipreparative HPLC (MeOH/H_2O, 80:20, *v*/*v*) to give compound **3** (4.06 mg, t_R = 30.55 min).

*Arthrichitin I (**1**).* light yellow powder. [α]24 D + 15.0 (*c* 0.1, MeOH); UV (MeOH) λ_{max} (log ε) 209 (1.78), 245 (0.75), 263 (0.53), 307 (0.63) nm; CD (*c* 7.5 × 10^{-4} mol/L, MeOH) λ_{max} ($\Delta\varepsilon$) 204 (−11.5), 214 (−0.7), 242 (−30.8), 261 (−8.2), 284 (−9.8), 314 (+20.4) nm; IR (KBr) ν_{max} 3318, 2925, 2855, 1741, 1662, 1518, 1435, 1365, 1245, 1174, 1039, 744 cm^{-1}; ^1H and ^{13}C NMR data see Table 1; HRESIMS *m*/*z* 737.3370 $[M + Na]^+$ (calcd. for $C_{36}H_{50}N_4O_{11}Na^+$, 737.3374).

*Arthrichitin J (**2**).* white powder. [α]24 D + 14.0 (*c* 0.1, MeOH); UV (MeOH) λ_{max} (log ε) 209 (2.18), 245 (0.98), 263 (0.71), 307 (0.84) nm; CD (*c* 7.5 × 10^{-4} mol/L, MeOH) λ_{max} ($\Delta\varepsilon$) 203 (−22.3), 212 (−1.8), 225 (−4.8), 238 (+4.6), 288 (−2.3), 312 (+6.8) nm; IR (KBr) ν_{max} 3326, 2925, 2854, 1726, 1638, 1514, 1436, 1374, 1242, 1210, 1093, 747 cm^{-1}; ^1H and ^{13}C NMR data see Table 1; HRESIMS *m*/*z* 673.3438 $[M + H]^+$ (calcd. for $C_{34}H_{49}N_4O_{10}^+$, 673.3449).

*Arthrichitin K (**3**).* light yellow powder. [α]24 D + 12.5 (*c* 0.1, MeOH); UV (MeOH) λ_{max} (log ε) 220 (2.10), 266 (0.51), 282 (0.44), 290 (0.44) nm; CD (*c* 7.5 × 10^{-4} mol/L, MeOH) λ_{max} ($\Delta\varepsilon$) 209 (−11.8), 228 (−1.7), 232 (−2.0), 252 (+0.5), 277 (+0.2), 312 (+1.8) nm; IR (KBr) ν_{max} 3289, 2923, 2854, 1736, 1648, 1541, 1438, 1382, 1240, 1174, 1045, 747 cm^{-1}; ^1H and ^{13}C NMR data see Table 1; HRESIMS *m*/*z* 643.3698 $[M + H]^+$ (calcd. for $C_{34}H_{51}N_4O_8^+$, 643.3707).

Marfey's Analysis for Compounds 1–3. The configuration of the amino acid residues in compounds **1**–**3** was determined by Marfey's analysis following acid hydrolysis.[21] Each compound (100 μg) was dissolved in 100 μL of 6 M HCl and hydrolyzed in pressure-resistant reaction flasks at 110 °C for 24 h. After hydrolysis, the HCl was removed by evaporation under a stream of N_2 gas. The hydrolysate was dissolved in 40 μL of 1 M $NaHCO_3$ (pH 7–8) and derivatized with 100 μL of 1% L-FDLA (1-fluoro-2,4-dinitrophenyl-5-L-leucinamide in acetone) at 40 °C for 1 h. The reaction mixture was neutralized to pH 2–3 with 40 μL of 1 M HCl, diluted with MeOH (840 μL), and filtered. Analysis was performed by UPLC-HRMS (Waters Xevo G2-S QTOF) using a linear gradient elution (20–50% solvent B over 15 min; solvent A: H_2O, solvent B: MeCN). Authentic samples of L-Ser, D-Trp, and D-Glu were separately derivatized with L-FDLA and D-FDLA, then analyzed under identical chromatographic conditions.

Computational Analysis. DP4+ probability analyses and ECD spectral calculations followed our established protocols.[24] The absolute configurations of **1**–**3** were assigned by statistical correlation of computed ^{13}C NMR chemical shifts and ECD spectra with experimental data sets.

Biological Assays. *Antibacterial Activities.* Antibacterial activity was assessed against five pathogenic bacteria, including the three Gram-positive bacteria methicillin-resistant *Staphylococcus aureus* (ATCC 43300), *Staphylococcus aureus* (ATCC 6538), and *Bacillus subtilis* (ATCC 21332) and the two Gram-negative bacteria *Vibrio parahemolyticus* (ATCC 17802) and *Escherichia coli* (ATCC 25922) by the agar disk-diffusion method.[25] All compounds were prepared in pure DMSO at 5 mg/mL and chloromycetin (positive control) was prepared at 0.5 mg/mL.

Cytotoxic Activity. Three human cancer cell lines (MHCC-97H, KTC-1, and DLD-1) were obtained from the Chinese Academy of Sciences (Shanghai, China). MHCC-97H and KTC-1 cells were cultured in DMEM medium (Solarbio, China), while DLD-1 cells were cultured in RPMI 1640 medium (Solarbio, China); all media were supplemented with 10% (*v*/*v*) fetal bovine serum (Sigma, USA) and under standard conditions (37 °C, 5% CO_2, humidified environment). Compounds **1**–**6** were tested at 40 μM concentration for cytotoxic effects using the MTT assay,[26] with Cisplatin serving as positive control (Selleck, China). For the assay, cells were seeded in 96-well plates (2.5 × 10^5 cells/well) and exposed to compound dilutions for 72 h. Following incubation, culture supernatant was carefully removed and replaced with 100 μL MTT solution (0.5 mg/mL) for 4–6 h at 37 °C. The supernatant was removed, and 100 μL of DMSO was added to each well. The absorbance was then measured at 490 nm using a microplate reader. All experiments were replicated thrice.

Antibenign Prostatic Hyperplasia Activity. RWPE-1 human prostate epithelial cell lines were provided by the Chinese Academy

https://doi.org/10.1021/acs.jnatprod.5c00752
J. Nat. Prod. 2025, 88, 2239–2246

of Sciences (Shanghai, China). The cells were cultured with Keratinocyte-SFM (K-SFM, Gibco, USA) containing 0.2% Gentamicin/Amphotericin Solution 500X (Gibco, USA) in a 37 °C, 5% CO_2 incubator. Cell viability assessment was conducted using the CCK-8 assay following established protocols.[27,28] Briefly, log-phase RWPE-1 cells were seeded into 96-well plates at a density of 5×10^3 cells/well. Each treatment group included eight replicate wells with varying compound concentrations. Following 48-h incubation, 10 μL CCK-8 reagent was added per well and incubated for 2−4 h. Absorbance at 450 nm was quantified using a microplate reader, with IC_{50} values derived from the resulting optical density measurements. All procedures strictly followed the manufacturer's guidelines for CCK-8 implementation.

■ ASSOCIATED CONTENT

Data Availability Statement

The NMR data for arthrichitins I−K have been deposited in the Natural Products Magnetic Resonance Database (NP-MRD; www.np-mrd.org) and can be found at NP0351137 (arthrichitin I), NP0351120 (arthrichitin J), and NP0351121 (arthrichitin K).

Supporting Information

The Supporting Information is available free of charge at https://pubs.acs.org/doi/10.1021/acs.jnatprod.5c00752.

^{1}H NMR, ^{13}C NMR, DEPT, HSQC, COSY, HMBC, NOESY spectra, and HRESIMS, ESI-MS/MS, UV, IR, Marfey's analysis, and ECD spectra of compounds **1**−**3** (PDF)

■ AUTHOR INFORMATION

Corresponding Authors

Cheng-Hai Gao − *Guangxi Key Laboratory of Marine Drugs and Institute of Marine Drugs, Guangxi University of Chinese Medicine, Nanning 530200, P.R. China; University Engineering Research Center of High-efficient Utilization of Marine Traditional Chinese Medicine Resources, Nanning 530200, P.R. China*; Email: gaoch@gxtcmu.edu.cn

Meng Bai − *Guangxi Key Laboratory of Marine Drugs and Institute of Marine Drugs, Guangxi University of Chinese Medicine, Nanning 530200, P.R. China; University Engineering Research Center of High-efficient Utilization of Marine Traditional Chinese Medicine Resources, Nanning 530200, P.R. China*; orcid.org/0000-0002-1024-3458; Email: XXBai2014@163.com

Authors

Yu Wang − *Institute of Marine Drugs, Guangxi University of Chinese Medicine, Nanning 530200, P.R. China*

Guang-Ping Cao − *Institute of Marine Drugs, Guangxi University of Chinese Medicine, Nanning 530200, P.R. China*

Xin-Jian Qu − *Guangxi Key Laboratory of Marine Drugs and Institute of Marine Drugs, Guangxi University of Chinese Medicine, Nanning 530200, P.R. China; University Engineering Research Center of High-efficient Utilization of Marine Traditional Chinese Medicine Resources, Nanning 530200, P.R. China*

Yong-Hong Liu − *Guangxi Key Laboratory of Marine Drugs and Institute of Marine Drugs, Guangxi University of Chinese Medicine, Nanning 530200, P.R. China; University Engineering Research Center of High-efficient Utilization of Marine Traditional Chinese Medicine Resources, Nanning 530200, P.R. China*; orcid.org/0000-0001-8327-3108

Xiang-Xi Yi − *Guangxi Key Laboratory of Marine Drugs and Institute of Marine Drugs, Guangxi University of Chinese Medicine, Nanning 530200, P.R. China; University Engineering Research Center of High-efficient Utilization of Marine Traditional Chinese Medicine Resources, Nanning 530200, P.R. China*; orcid.org/0000-0002-8251-8836

Complete contact information is available at: https://pubs.acs.org/10.1021/acs.jnatprod.5c00752

Author Contributions

Y.W. and G.-P.C. contributed equally.

Notes

The authors declare no competing financial interest.

■ ACKNOWLEDGMENTS

This work was supported by the Natural Science Foundation of Guangxi (2023GXNSFAA026313), Guangxi key research and development program (AB24010109), Guangxi University of Traditional Chinese Medicine Outstanding Young Scholars Fund Project (2024JQ001), The Development Program of High-level Talent Team under the Qihuang Project of Guangxi University of Chinese Medicine (202404).

■ REFERENCES

(1) Aly, A. H.; Debbab, A.; Proksch, P. *Pharmazie.* **2013**, *68*, 499−505.

(2) Gao, H.; Li, G.; Lou, H.-X. *Molecules.* **2018**, *23*, 646.

(3) Poynton, E. F.; van Santen, J. A.; Pin, M.; Contreras, M. M.; McMann, E.; Parra, J.; Showalter, B.; Zaroubi, L.; Duncan, K. R.; Linington, R. G. *Nucleic. Acids. Res.* **2025**, *53*, D691−D699.

(4) Netzker, T.; Flak, M.; Krespach, M. K.; Stroe, M. C.; Weber, J.; Schroeckh, V.; Brakhage, A. A. *Curr. Opin. Microbiol.* **2018**, *45*, 117−123.

(5) Oh, D. C.; Kauffman, C. A.; Jensen, P. R.; Fenical, W. *J. Nat. Prod.* **2007**, *70*, 515−520.

(6) Marmann, A.; Aly, A. H.; Lin, W.; Wang, B.; Proksch, P. *Mar Drugs.* **2014**, *12*, 1043−1065.

(7) Ueda, K.; Beppu, T. *J. Antibiot.* **2017**, *70*, 361−365.

(8) Li, Y. Z.; Zhang, W. Q.; Hu, P. F.; Yang, Q. Q.; Molnár, I.; Xu, P.; Zhang, B. B. *Nat. Prod. Rep.* **2025**, *42*, 623−637.

(9) Chagas, F. O.; Dias, L. G.; Pupo, M. T. *J. Chem. Ecol.* **2013**, *39*, 1335−1342.

(10) Bertrand, S.; Bohni, N.; Schnee, S.; Schumpp, O.; Gindro, K.; Wolfender, J. L. *Biotechnol. Adv.* **2014**, *32*, 1180−1204.

(11) Wang, Y.; Cao, G. P.; Gan, Y. M.; Lin, X.; Yi, X. X.; Zhao, L. Y.; Liu, Y. H.; Gao, C. H.; Bai, M. *Mar. Drugs.* **2024**, *22*, 282.

(12) Xu, C.; Cao, G. P.; Zhang, H.; Bai, M.; Yi, X. X.; Qu, X. J. *Mar. Drugs.* **2024**, *22*, 275.

(13) He, J. L.; Jiang, X. D.; Gan, Y. M.; Qu, X. J.; Yi, X. X.; Liu, Y. H.; Gao, C. H.; Bai, M. *Nat. Prod. Res.* **2024**, 1−7.

(14) Knowles, S. L.; Raja, H. A.; Isawi, I. H.; Flores-Bocanegra, L.; Reggio, P. H.; Pearce, C. J.; Burdette, J. E.; Rokas, A.; Oberlies, N. H. *Org. Lett.* **2020**, *22*, 1878−1882.

(15) Hwang, G. J.; Jang, M.; Son, S.; Kim, G. S.; Lee, B.; Heo, K. T.; Kim, G. J.; Choi, H.; Hur, J. S.; Jang, J. P.; Ko, S. K.; Hong, Y. S.; Ahn, J. S.; Jang, J. H. *J. Nat. Prod.* **2022**, *85*, 2445−2453.

(16) Peng, X. Y.; Wu, J. T.; Shao, C. L.; Li, Z. Y.; Chen, M.; Wang, C. Y. *Mar. Life Sci. Technol.* **2021**, *3*, 363−374.

(17) Xu, S.; Li, M. S.; Hu, Z.; Shao, Y. L.; Ying, J. L.; Zhang, H. W. *Microorganisms.* **2023**, *11*, 464.

(18) Wang, Z. J.; Hong, Y. R.; Wang, X. Y.; Wang, J. Z.; Zhai, Y. J.; Cui, W.; Han, W. B. *J. Nat. Prod.* **2024**, *87*, 2180−2193.

(19) Mai, V. H.; Choi, S.; Ponce-Zea, J. E.; Nguyen, T. T. T.; Kang, H. S.; Yang, H. J.; Lee, H. B.; Oh, W. K. *J. Nat. Prod.* **2025**, *88*, 384−396.

(20) Helaly, S. E.; Ashrafi, S.; Teponno, R. B.; Bernecker, S.; Dababat, A. A.; Maier, W.; Stadler, M. *J. Nat. Prod.* **2018**, *81*, 2228−2234.

(21) Lin, X.; Tang, Z.; Gan, Y.; Li, Z.; Luo, X.; Gao, C.; Zhao, L.; Chai, L.; Liu, Y. *J. Nat. Prod.* **2023**, *86*, 994−1002.
(22) Liu, F.; Qiao, X.; Li, Q.; Zhou, J.; Gao, J.; He, F.; Wu, P.; Chen, C.; Sun, W.; Zhu, H.; Zhang, Y. *J. Nat. Prod.* **2024**, *87*, 753−763.
(23) Yuan, S.; Zhuang, S.; Qiao, Y.; Wu, Q.; Ma, Y.; Chen, S.; Liu, L.; Yan, Y.; Gao, Z. *J. Nat. Prod.* **2025**, *88*, 1605−1615.
(24) Xia, J. L.; Liu, J. Y.; Liu, K.; Li, Y. Y.; Bai, M.; Gao, C. H.; Yi, X. X. *J. Nat. Prod.* **2025**, *88*, 1980−1987.
(25) Balouiri, M.; Sadiki, M.; Ibnsouda, S. K. *J. Pharm. Anal.* **2016**, *6*, 71−79.
(26) Mosmann, T. *J. Immunol. Methods.* **1983**, *65*, 55−63.
(27) Choi, Y. J.; Fan, M.; Wedamulla, N. E.; Tang, Y. J.; Kim, E. K. *Food Sci. Hum. Well.* **2024**, *13*, 1698−1710.
(28) He, J. L.; Wang, Y.; Yi, X. X.; Gan, Y. M.; Liu, Y. H.; Gao, C. H.; Liu, K.; Bai, M. *J. Nat. Prod.* **2025**, *88*, 1201−1207.

https://doi.org/10.1021/acs.jnatprod.5c00752
J. Nat. Prod. 2025, 88, 2239−2246